HHS Public Access

Author manuscript

Circ Res. Author manuscript; available in PMC 2020 January 04.

Published in final edited form as:

Circ Res. 2019 January 04; 124(1): 79–93. doi:10.1161/CIRCRESAHA.118.313854.

ATF6 Regulates Cardiac Hypertrophy by Transcriptional Induction of the mTORC1 Activator, Rheb

Erik A. Blackwood[1], **Christoph Hofmann**[1,2,3], **Michelle Santo Domingo**[1], **Alina S. Bilal**[1], **Anup Sarakki**[1], **Winston Stauffer**[1], **Adrian Arrieta**[1], **Donna J. Thuerauf**[1], **Fred W. Kolkhorst**[1], **Oliver J. Müller**[2,3,4], **Tobias Jakobi**[3,5], **Christoph Dieterich**[3,5], **Hugo A. Katus**[2,3], **Shirin Doroudgar**[2,3], and **Christopher C. Glembotski**[1]

[1]San Diego State University Heart Institute and the Department of Biology, San Diego State University, San Diego, CA 92182

[2]Department of Cardiology, Angiology, and Pneumology, University Hospital Heidelberg, Innere Medizin III, Im Neuenheimer Feld 669, 69120 Heidelberg, Germany

[3]DZHK (German Centre for Cardiovascular Research), Partner Site Heidelberg/Mannheim, 69120 Heidelberg, Germany

[4]Department of Internal Medicine III, University of Kiel, Arnold-Heller-Str.3, Kiel, Germany

[5]Section of Bioinformatics and Systems Cardiology, Department of Internal Medicine III, Klaus Tschira Institute for Integrative Computational Cardiology, University Hospital Heidelberg, Heidelberg, Germany

Abstract

Rationale: ER stress dysregulates ER proteostasis, which activates the transcription factor, ATF6, an inducer of genes that enhance protein folding and restore proteostasis. Due to increased protein synthesis, it is possible that protein folding and, thus, ER proteostasis are challenged during cardiac myocyte growth. However, it is not known whether ATF6 is activated, and if so, what its function is during hypertrophic growth of cardiac myocytes.

Objective: To examine the activity and function of ATF6 during cardiac hypertrophy.

Methods and Results: We found that ATF6 was activated and ATF6-target genes were induced in mice subjected to an acute model of trans-aortic constriction (TAC), or to free-wheel exercise, which promote adaptive cardiac myocyte hypertrophy with preserved cardiac function. Cardiac myocyte-specific deletion of *Atf6* (ATF6 cKO) blunted TAC- and exercise-induced cardiac myocyte hypertrophy and impaired cardiac function, demonstrating a role for ATF6 in compensatory myocyte growth. Transcript profiling and chromatin immunoprecipitation identified *RHEB* as an ATF6-target gene in the heart. RHEB is an activator of mTORC1, a major inducer of protein synthesis and subsequent cell growth. Both TAC and exercise upregulated *RHEB*, activated

Address correspondence to: Dr. Christopher C. Glembotski, SDSU Heart Institute and Department of Biology, San Diego State University, 5500 Campanile Drive, San Diego, CA 92182,USA, Tel.: (619) 594-2959, FAX: (619) 594-5676, cglembotski@mail.sdsu.edu.

DISCLOSURES

None.

mTORC1, and induced cardiac hypertrophy in WT mouse hearts, but not in ATF6 cKO hearts. Mechanistically, knockdown of ATF6 in neonatal rat ventricular myocytes blocked phenylephrine (PE)-, and insulin-like growth factor 1 (IGF1)-mediated *Rheb* induction, mTORC1 activation, and myocyte growth, all of which were restored by ectopic RHEB expression. Moreover, AAV9-*RHEB* restored cardiac growth to ATF6 cKO mice subjected to TAC. Finally, ATF6 induced *RHEB* in response to growth factors, but not in response to other activators of ATF6 that do not induce growth, indicating that ATF6 target gene induction is stress-specific.

Conclusions: Compensatory cardiac hypertrophy activates ATF6, which induces *Rheb* and activates mTORC1. Thus, ATF6 is a previously unrecognized link between growth stimuli and mTORC1-mediated cardiac growth.

Keywords

Myocytes; cardiac protein folding; proteostasis; cardiac hypertrophy; ATF6; Rheb; mTORC1; ER stress; Basic Science Research

INTRODUCTION

Protein homeostasis, or proteostasis involves the coordination of protein synthesis and folding to ensure proteome integrity and vital cell function[1]. In cardiac myocytes the endoplasmic reticulum (ER) is a major site of synthesis of proteins that are critical for proper function of the heart, including many calcium-handling proteins, receptors, and secreted proteins, such as hormones, stem cell homing factors, and growth factors[2, 3]. Therefore, ER proteostasis maintains the integrity of the cardiac myocyte proteome and, thus, cardiac contractility. Increased protein synthesis in growing cardiac myocytes must be balanced by increased protein-folding to avoid the accumulation of toxic misfolded proteins; thus growth poses a potential challenge to cardiac myocyte proteostasis[4]. However, the molecular mechanisms underlying the maintenance of ER proteostasis during cardiac myocyte growth are not well understood.

ER proteostasis is controlled in all mammalian cells by several ER-transmembrane sensors of protein misfolding, including the adaptive transcription factor, ATF6[5]. When protein synthesis surpasses the capacity of the protein-folding machinery, increases in misfolded proteins cause the translocation of the ER-transmembrane, 670-amino acid, 90 kD form of ATF6, to the Golgi, where it is clipped, liberating an N-terminal fragment that serves as a transcription factor. This 50 kD active form of ATF6 regulates a gene program that is responsible for the expression of numerous proteins that enhance ER protein folding, which adaptively restores the balance between protein synthesis and folding[6, 7]. Thus, nodal proteostasis regulators, such as ATF6, that sense and maintain this balance could play important roles in optimizing cardiac myocyte growth; however, neither the activation nor the function of ATF6 in the setting of hypertrophic cardiac growth has been examined. Accordingly, here we studied the effects of *Atf6* deletion in mouse hearts and in cultured cardiac myocytes during physiologically-relevant maneuvers known to promote compensatory cardiac hypertrophy in either a concentric (pressure overload)[8] or eccentric (exercise)[9] manner, positing that the absence of ATF6 would imbalance proteostasis, which would be maladaptive.

Both growth maneuvers activated ATF6, and *Atf6* deletion was maladaptive, as evidenced by impaired cardiac function. However, surprisingly, cardiac myocyte growth was also impaired upon *Atf6* deletion. This was unexpected, since *Atf6* is not known to be required for cardiac myocyte growth. Further mechanistic studies showed that ATF6 is activated as a result of the increased demands placed on the ER protein folding machinery during growth-related increases in protein synthesis. Moreover we found that *Atf6* serves a previously unrecognized role as a molecular link between growth stimuli and activation of mammalian/mechanistic target of rapamycin complex 1 (mTORC1), a major promoter of protein synthesis and consequent growth of cardiac myocytes[10–15]. Two conditions need to be met for mTORC1 to be activated; 1) in response to a growth stimulus, mTORC1 needs to translocate to organelles, such as lysosomes[16], where it encounters the small GTPase activator of mTORC1, Rheb[17], and 2) Rheb must be active and present in sufficient quantities[18]. In terms of Rheb activation, it is known that growth stimuli lead to the phosphorylation and, thus, inhibition of the Rheb GTPase-activating protein (GAP), TSC1/TSC2[19], which increases the GTP-loading state and, thus, the activity of Rheb. However, the molecular mechanisms underlying the *Rheb* gene expression are less well understood. Here, we showed, for the first time, that ATF6 is an inducer of *Rheb*, and in this way, ATF6 coordinates protein synthesis and protein folding, ensuring the adaptive maintenance of proteostasis in growing cardiac myocytes. Thus, ATF6 is a newly identified and essential member of mTORC1 growth signaling in cardiac myocytes in the heart.

METHODS

All supporting data are available within the article. Further details on the Methods can be found in the Online Supplement.

Laboratory animals.

The research reported in this paper has been reviewed and approved by the SDSU Institutional Animal Care and Use Committee and it conforms to the Guide for the Care and Use of Laboratory Animals published by the National Research Council.

ATF6 floxed mice.

Atf6α$^{fl/fl}$ mice used in this study were generated by Dr. Gokhan S. Hotamisligil[20]. All of the mice used in this study were 10 week-old males.

Statistics.

Unless otherwise stated, values shown are mean ± SEM and statistical treatments are either a t-test or a one-way ANOVA followed by Newman-Keuls *post hoc* analysis.

RESULTS

ATF6 is required for cardiac myocyte hypertrophy in response to pressure overload.

To examine the role of *Atf6* in cardiac myocytes on heart growth, we generated an *Atf6* conditional knockout mouse (ATF6 cKO) by injecting *Atf6*$^{fl/fl}$ mice with a recombinant AAV9 that encodes *Cre* under the control of the *cardiac troponin T* promoter (Fig. 1A).

Compared to *Atf6*$^{fl/fl}$ injected with AAV9-Con, injection with AAV9-CRE effectively reduced *Atf6* mRNA from cardiac myocytes isolated from *Atf6*$^{fl/fl}$ mice, but not non-cardiac myocytes, or liver (Fig. 1B). *Atf6*$^{fl/fl}$ mice injected with AAV9-Con (Con) or AAV9-CRE (ATF6 cKO), were subjected to TAC and examined 7d later, when hypertrophic growth is maximal[21] and structural remodeling is compensatory[22, 23]. TAC activated ATF6 in Con mouse hearts, as evidenced by increased levels of the active, 50 kD form of ATF6 (Fig. 1C). This was unexpected, since ATF6 is not known to be activated in cardiac myocytes by any growth stimulus. Coordinate with ATF6 activation, TAC increased expression of numerous canonical ATF6 target genes (Fig. 1C-D; Online Fig. IA). As expected, ATF6 was undetectable in ATF6 cKO mouse hearts (Fig. 1C-D). TAC increased Con mouse heart weights, but, surprisingly, this growth effect was significantly blunted in ATF6 cKO mouse hearts (Fig. 1E). TAC increased *Nppa and Nppb* expression to similar extents in both Con and ATF6 cKO mice, while the induction of *Myh7* and *Col1a1* was slightly greater in the ATF6 cKO mice (Fig. 1F). This, coupled with the decrease in *Atp2a2* i.e. *SERCA2a* in ATF6 cKO mice, suggests a blunted compensatory response in the absence of ATF6. In Con mouse hearts, cardiac function, including fractional shortening was preserved, while chamber dimensions were unchanged after TAC (Fig. 1G; Online Table I) and cardiac myocyte size was increased (Fig. 1H), consistent with the compensatory nature of cardiac hypertrophy in mice at this time after pressure overload[24]. However, in contrast to Con, in ATF6 cKO mice subjected to TAC myocyte size was decreased compared to Con (Fig. 1H) and fractional shortening was impaired (Fig. 1G) with increased chamber dimensions, such as LVEDV and LVESV, despite high frequency Doppler measurements between right and left carotid arteries demonstrating consistent and identical pressure overload in TAC-operated Con and ATF6 cKO mice (Online Table I). Along with increased plasma levels of cTnI (Online Fig. IB), these results are consistent with the initial stages of chamber dilation, as well as myocardial damage and decompensation in the ATF6 cKO mice. Thus, ATF6 is activated by pressure overload and is required for hypertrophy.

ATF6 is required for cardiac myocyte hypertrophy in response to exercise.

To assess the breadth of the impact of ATF6 on heart growth, we examined the effects of cardiac myocyte-specific ATF6 deletion in mice subjected to free-wheel exercise[25, 26] (Fig. 2A). Similar to TAC, exercise surprisingly activated ATF6 and induced ATF6 target genes in Con, but not in ATF6 cKO mice (Fig. 2B-C). As expected, compared to Con sedentary mice, Con mice subjected to exercise exhibited increased heart weights and LV wall thickness, as well as myocyte size (Fig. 2D, 2F; Online Table II). While *Nppa* and *Nppb* were mildly increased, *Atp2a2* was robustly increased by exercise in Con mouse hearts, and there was no change in *Myh7* or *Col1a1* (Fig. 2E); this gene profile is typical of adaptive cardiac hypertrophy in exercising mice[24, 27]. In contrast to Con, in ATF6 cKO mice subjected to exercise there was no change in heart weights or LV wall thickness (Fig. 2D; Online Table II), reduced increases in myocyte size (Fig. 2F), and reduced induction of ATF6 target genes (Fig. 2C). Compared to exercised Con mice, exercised ATF6 cKO mice showed no increase in *Nppa*, and neither Con nor ATF6 cKO mice showed significant changes in *Nppb* or *Myh7*. Importantly, while Con mice exhibited decreased *Col1a1* and increased *Atp2a2* after exercise, which are beneficial genetic changes typical of this regime, the ATF6 cKO mice

failed to adapt and had increased *Col1a1* and no change in *Atp2a2* (Fig. 2E). Thus, ATF6 is activated by exercise and is required for compensatory hypertrophy in this exercise model.

Rheb is an ATF6-inducible gene in the heart.

Since there are no known *Atf6*-inducible genes that are required for cardiac myocyte growth, we turned to transcript profiling for clues to the identities of such genes. RNA sequencing of the hearts of our previously published transgenic mice that express activated ATF6[28] (Online Table III) revealed that ATF6 induced 51 genes in the gene ontology category, small GTPase mediated signal transduction; this category includes the ras-related small GTPase, Ras homologue enriched in brain (*RHEB*) (Fig. 3A; Online Fig. IIA). Rheb is required for activation of mTORC1, however, only in the presence of a growth stimulus. Accordingly, we focused on *Rheb* as a candidate gene through which ATF6 might contribute to cardiac hypertrophy, pursuing the hypothesis that increased *Rheb* gene expression and subsequent mTORC1 activation under growth conditions are *Atf6*-dependent. The upregulation of *RHEB* by ATF6 in mouse hearts observed by RNA sequencing was confirmed by qRT-PCR (Online Fig. IIB). Consistent with ATF6 as a possible transcriptional inducer of *Rheb* was our finding that the *Rheb* promoter has two potential ATF6 binding sites, which we call ER stress response elements (ERSEs)-1 and −2 (Fig. 3B). Chromatin immunoprecipitation (ChIP) showed that ATF6 binds to both sites in the *RHEB* gene in neonatal rat ventricular myocytes (NRVM) (Fig. 3C). The progressive decline in *RHEB* promoter activity in plasmids that encode 5'-truncation deletions of the rat *RHEB* promoter driving luciferase demonstrated the importance of these putative ERSEs in ATF6-mediated *RHEB* promoter activation (Online Fig. IIC). To mechanistically investigate the functional involvement of these ERSEs further, we mutated either or both ERSE (Fig. 3D). Mutating either ERSE decreased ATF6 *RHEB* promoter activation by ATF6, however, the promoter-proximal site, i.e. ERSE-1 appeared to have the largest effect (Fig. 3E). To determine whether ATF6 is sufficient to induce *Rheb* in the heart, *in vivo*, mice were injected with a recombinant AAV9 that encodes activated ATF6, i.e. ATF6(1–373). qRT-PCR and immunoblotting demonstrated that activated ATF6 increased *RHEB* mRNA and protein in the heart (Online Fig. IID-F). These results are the first demonstration in any cell type that ATF6 induces *RHEB,* implicating ATF6 as a critical link between growth stimuli and mTORC1 activation.

RHEB induction during pressure-overload and exercise requires ATF6.

We found that *RHEB* was strongly induced in Con mice after either TAC or exercise, but not in ATF6 cKO mouse hearts (Fig. 3F-K). Thus, ATF6 is necessary for the upregulation of RHEB in these models of cardiac hypertrophy, *in vivo*. Since RHEB is required for mTORC1 activation in response to a growth stimulus, we assessed mTORC1 pathway activation. As expected, pressure-overload and exercise both activated mTORC1, as shown by increased phosphorylation of mTORC1 (Ser2448), p70 ribosomal S6 kinase (S6K; Thr389), and eukaryotic translation initiation factor 4E-binding protein 1 (4E-BP1; Thr37/46); however, mTORC1 activation was blunted in ATF6 cKO mouse hearts (Fig. 3G, J), consistent with the key role for ATF6 in mTORC1 activation by growth stimuli. To examine whether ATF6 might affect other signaling pathways leading to mTORC1 activation, we assessed the phosphorylation of Akt on Ser308 and the phosphorylation of TSC2, both of which lie upstream of Rheb in the mTORC1 signaling pathway. We found

that pressure overload increased phosphorylation of Akt (Thr308) and TSC2 (Thr1462), as expected; however, in contrast to Rheb expression, neither of these phosphorylation events were affected by *ATF6* deletion (Online Fig. IIIA). Thus, the deficit in mTORC1 activation in ATF6 cKO mice must reside downstream of Akt and TSC2, i.e. Rheb. We also examined whether ATF6 deletion affected other well known canonical hypertrophy signaling pathways, but found that neither phosphorylation of Akt on Ser473, Erk phosphorylation (Online Fig. IIIA) or calcineurin activation (Online Fig. IIIB) were affected by ATF6 deletion. These results pinpoint the growth deficit in the ATF6 cKO mouse hearts to the inability to upregulate Rheb.

RHEB is required for PE- and IGF1-induced cardiac myocyte growth.

To explore the mechanistic relationship between *ATF6* and *RHEB* we used *RHEB* and *ATF6* loss-of-function approaches in NRVM treated with the α_1-adrenergenic receptor agonist, phenylephrine (PE) or insulin-like growth factor 1 (IGF1), which recapitulate much of the intracellular signaling during pressure-overload or exercise-induced hypertrophy, respecitvely[29]. Knocking down either *ATF6* or *RHEB* abrogated the effects of PE or IGF1 on cardiac myocyte hypertrophy, fetal gene induction, ATF6 target gene induction and mTORC1 signaling (Fig. 4A-E; Online Fig. IVA, IVC; Fig. 5A-E; Online Fig. IVB), but had no effect on mTORC2 signaling, as assessed by phosphorylation of Akt on Ser-473 (Online Fig. IVD-E). To further substantiate the results with *Rheb* siRNA, we used a different Rheb loss-of-function approach involving the Rheb inhibitor, Lonafarnib[30]. Lonafarnib mimicked the effects of *Rheb* siRNA on PE- and IGF1-mediated ATF6 activation, mTORC1 signaling, ATF6 gene induction and growth in NRVM (Online Fig. V).

To complement *ATF6* loss-of-function approach, we used a gain-of-function approach, examining the effects of ectopic expression of *ATF6* and *RHEB*. In the absence of a growth stimulus, ectopic expression of *ATF6* did not increase myocyte growth, as expected, due to the absence of mTORC1 activation under these conditions (Online Fig. VIA Con). Either PE or IGF1 increased myocyte growth, which was completely blocked by the mTORC1 inhibitor, rapamycin, as expected (Online Fig. VIA, PE and IGF1, red vs blue). Ectopic ATF6 augmented the growth-promoting effects of PE and IGF1, which were also completely blocked by rapamycin (Online Fig. VIA, PE and IGF1, black and green). Moreover, ectopic ATF6 slightly augmented PE- and IGF1-stimulated NRVM growth, however, it was not able to restore growth in cells treated with either *RHEB* siRNA or Lonafarnib (Online Fig. VIB-C). As expected, ectopic expression of *RHEB* had no effect in the absence of a growth stimulus; however, upon a growth stimulus, the loss of growth and mTORC1 activation seen with *ATF6* siRNA were completely restored by ectopically expressed *RHEB* (Fig. 4F-H; Fig. 5F-H).

Mechanistic relationship between growth signaling and the UPR.

The unfolded protein response (UPR), which in addition to ATF6, is mediated by PERK and IRE1[5], is activated by the misfolding of proteins induced by a variety of chemical and pathophysiological treatments, most of these do not promote growth. In fact, the UPR is not widely considered to be growth-promoting. Accordingly, since we found here that ATF6 can be activated during growth, we assessed how growth affected the other arms of the UPR. We

found that PE and IGF1 activated all three arms of the UPR in a rapamycin-sensitive manner (Online Fig. VIIA), indicating that mTORC1 activation is required for UPR activation during growth. We then individually knocked down *ATF6, PERK* and *IRE1*, and found that only ATF6 knockdown blunted growth (Online Fig. VIIB-C). To ensure that the effects of ATF6 on growth are dependent on the transcriptional effects of ATF6, we showed that NRVM infected with AdV-ATF6(1–373) [active] exhibited increased growth in response to PE, especially when endogenous ATF6 was knocked down, however AdV-ATF6(94–373) [trancriptionally inactive] did not (Online Fig. VIID).

Next, we examined the effect on mTORC1 signaling of other UPR stimulators that do not affect growth, such as tunicamycin (TM), which increases ER protein misfolding by inhibiting protein glycosylation in the ER. In contrast to PE, activation of ATF6 by TM was not dependent on *RHEB* (Fig. 6A-B). Additionally, while *RHEB* knockdown blocked PE- and IGF1-mediated induction of ATF6 target genes, (Fig. 4E, 5E), it had no effect on TM-mediated induction of ATF6 target genes (Fig. 6C). Thus, there are RHEB/growth-dependent and RHEB/growth-independent pathways that lead to ATF6 activation and induction of ATF6 target genes.

Stimulus-dependent differential induction of ATF6 target genes.

We dived deeper into the mechanism of RHEB/growth-dependent and RHEB/growth-independent pathways of ATF6 activation. We previously showed that ATF6 induces some proteins targeted to the ER, where they enhance protein folding (e.g. *HSPA5*/*GRP78*), and others located outside the ER, where they serve other functions. One example of the latter is our finding that I/R activates ATF6-dependent induction of *catalase (CAT)*, which resides in peroxisomes and neutralizes damaging ROS. Here, we provide an additional example of an ATF6-inducible gene, *RHEB*, that encodes a protein that resides outside the ER. Because of the differences in the locations and functions of Hspa5, Cat, and Rheb, we posited that they might be differentially induced by treatments that cause ER protein misfolding (TM), or oxidative stress (I/R) but do not induce growth, or to a treatment that induces growth (PE). While, for the most part, the mRNA levels for all three genes were increased by all the treatments, the quantitative nature of induction differed depending on the treatments, such that TM, sI/R, and PE had the greatest effects on induction of *Hspa5, Cat,* and *Rheb,* respectively (Fig. 6D). Notably, *CAT* induction was highly selective, showing an approximate 6-fold induction by sI/R, and much less induction by either TM or PE (Fig. 6D, *Cat*). Remarkably, *RHEB* induction was also highly selective, showing the least induction by TM or sI/R, while being induced by over 5-fold by PE (Fig. 6D, *Rheb*). Importantly, all of these effects depended on ATF6 (Fig. 6E).

To dissect this stimulus-dependent differential gene induction further, we showed that promoter/luciferase reporter constructs for *Hspa5, Cat,* and *Rheb* (Fig. 6F) were also differentially induced by TM, sI/R and PE, mimicking mRNA induction (Fig. 6G). Importantly, as with the mRNA, all of these effects depended upon ATF6 (Fig. 6H).

These stimulus-specific effects of ATF6 on *Hspa5, Cat,* and *Rheb* could be due to the stimulus-dependent binding of ATF6 to the ERSEs in these genes. To test this, we developed a new method for measuring ATF6 binding to the *HSPA5, CAT,* and *RHEB* promoters in

cells treated with TM, sI/R or PE. To this end we generated a recombinant AdV FLAG full-length p90 ATF6, i.e. ATF6(1–670), which remains in the ER in the absence of ER stress, and, therefore, can not bind to ERSEs. NRVM expressing FLAG-ATF6(1–670) were treated with TM, sI/R or PE, each of which induce the formation of the FLAG-tagged N-terminal, active p50 form of ATF6, so it can bind to ERSEs. ChIP demonstrated that the binding of ATF6 to these genes differed, depending on the stimulus, mimicking the mRNA induction and promoter activation (Fig. 6I). These effects were not seen with AdV encoding only FLAG, verifying ATF6-specificity (Fig. 6J). This shows, for the first time in any cell type, that ATF6 can be activated by a broad spectrum of conditions that affect proteostasis in a variety of ways, yet the relative induction of ATF6 targets differs in a condition-dependent manner.

Ectopic expression of RHEB restores cardiac growth to ATF6 cKO mouse hearts.

Next, we assessed the effects of ectopic expression of *RHEB* in the heart, *in vivo* using a new recombinant AAV9-RHEB (Fig. 7A). In ATF6 cKO mice, AAV9-RHEB effectively restored the loss of mTORC1 signaling, hypertrophic growth and cardiac function, as well as the hypertrophic and ATF6 gene programs in response to TAC (Fig. 7B-F; Online Table IV). Thus, it is by increasing RHEB that ATF6 influences mTORC1 signaling and subsequent cardiac myocyte growth, fetal gene expression and ATF6-target gene expression.

ATF6 activation in response to growth requires mTORC1 activation, protein synthesis and protein misfolding.

To this point, mTORC1 and ATF6 activation were shown to be dependent on each other under the growth conditions examined. To account for this interdependence, we posited a temporal sequence of events, wherein the initial event is mTORC1 activation, which depends on basal levels of Rheb (Fig. 8A, Step 1). This initial mTORC1 activation precedes, but drives initial increases in protein synthesis that place demands on the protein-folding machinery (Fig. 8A, Step 2), which activates ATF6. Then, ATF6 serves canonical- and non-canonical roles (Fig. 8A, Steps 3, 4), the latter of which includes *RHEB* induction (Fig. 8A, Step 5), which is necessary to sustain mTORC1 activation (Fig. 8A, Step 6) and the continued increases in protein synthesis that required for growth and cardiac myocyte hypertrophy (Fig. 8A, Step 7). To examine this hypothesis, a TAC time course was carried out. At 3h of TAC, a time when mTORC1 is activated, but protein synthesis has not yet increased, mTORC1 signaling was activated, but ATF6 was not activated and *RHEB* was not induced (Fig. 8B, 3h). However, at both 2 and 7d of TAC, when protein synthesis is increased, mTORC1 signaling and ATF6 were activated, and *RHEB* was induced (Fig. 8B, 2d and 7d). As expected, heart weights increased as a function of TAC time from 3h to 7d (Fig. 8C; Online Table V). Thus, mTORC1 activation occurred soon after TAC and preceded ATF6 activation. Further supporting our hypothesis that initially, mTORC1 activation precedes ATF6 activation were results of a 3h TAC experiment in ATF6 cKO mice, where, in contrast to longer times of TAC (i.e. 7d - Fig. 3G), the deletion of ATF6 did not affect mTORC1 activation (Fig. 8D). As expected, heart weights did not change under these conditions (Fig. 8E; Online Table VI).

Consistent with these results, when examining the effect of PE and IGF1 at the earliest time points, just prior to when protein synthesis is greatest in NRVM, knocking down *ATF6* did not affect mTORC1 activation (Online Fig. VIIIA), but again, ATF6 activation was rapamycin-dependent (Online Fig. VIIIB). Moreover, inhibiting protein synthesis with cycloheximide had no effect on mTORC1 activation at these short times of PE or IGF1 treatment, but impaired ATF6 activation and *RHEB* induction, indicating that protein synthesis is required for ATF6 activation and subsequent *RHEB* induction (Online Fig. VIIIC). Finally, in NRVM treated with the chemical chaperone, 4PBA, PE and IGF1 activated mTORC1 however, ATF6 was not activated and *RHEB* was not induced (Online Fig. VIIID), indicating the increase in protein folding demand driven by increases in protein synthesis are responsible for activating ATF6.

DISCUSSION

ATF6 is required for growth of the heart.

While previous studies reported increased expression of a few ER stress genes in mouse models of pressure overload, implicating ER protein misfolding[31–34], prior to our study here, neither the activation nor the roles for ATF6 in cardiac myocytes during cardiac growth had been examined. Here, we showed, for the first time that ATF6, a major mediator of the UPR, is activated by diverse growth stimuli and that ATF6 is required for growth of the heart in response to these stimuli. We determined that the mechanism of this effect involves ATF6-mediated induction of *RHEB* (Fig. 8A). It was surprising to find that ATF6 is required for heart growth, considering the UPR is not widely known to be involved in growth processes. However, this non-canonical role for ATF6 complements its canonical role as a sensor of misfolded proteins in the ER and, as such, a sensor of increases in protein folding demand, which occur during growth. Thus, ATF6 maintains proteostasis and proteome integrity when the heart is stimulated to grow in a compensatory manner.

ATF6 exhibits stress-specific transcriptional gene induction.

We also found that, depending on the stimulus, ATF6 target genes are differentially expressed due to the unique effects that the stresses have on ATF6 binding to, and thus, transcriptional activation of ATF6 target genes. Such differential ATF6 target gene induction by treatments that all activate ATF6 suggests that there are yet-to-be-described regulatory layers that fine-tune the ATF6 gene program to best adapt to the conditions. Some possible mechanisms that could contribute to this differential expression are beginning to emerge, as it has been shown that ATF6 can interact with other transcription factors, such as Nrf1, PGC1α and β, and ERRγ,[35–37] which changes the transcriptional programming in ways that fine-tune ATF6 target gene induction. Additionally, it was recently shown that ATF6 can be differentially activated by lipids and proteotoxic stress at least partly by virtue of separate activation domains on ATF6 for these two different stresses[38].

Rheb in the heart.

Rheb was originally documented as an mTORC1 activator in the brain[39], this role has been demonstrated in numerous other tissues and organs[17, 40, 41]. Global deletion of *Rheb* is embryonic lethal, in part due to cardiac defects[42], demonstrating the importance of Rheb-

mediated mTORC1 activation in heart growth and development. The growth-promoting effect of *Rheb* gain-of-function was demonstrated in adult rat ventricular myocytes transfected with adenovirus encoding *Rheb*[43]. However, overexpression of *Rheb* in transgenic mice increased infarct size, in part because Rheb inappropriately decreased autophagy, which is adaptive in this disease setting[44]. Pharmacological inhibition of Rheb in mice subjected to TAC for three weeks was cardioprotective[14]. These findings differ from our study, perhaps because different times after TAC were studied, or different approaches to decreasing Rheb. It is also possible that Rheb induction and mTORC1 activation have different roles in a severe afterload-induced hypertrophy model, such that acute activation works in a compensatory manner, but chronic activation drives decompensation. The αMHC-CRE-dependent conditional deletion of *Rheb* from mouse cardiac myocytes resulted in atrophic hearts, heart failure, and death within 1–2 weeks after birth, a timeframe that aligns with the time of αMHC expression after birth[12, 45]. Although there have been no studies prior to ours mechanistically connecting *Atf6* with *Rheb* induction, one study in tumor cells[46], and another in the setting of Huntington's disease[47], have implicated such a connection and, therefore, support the findings reported here.

Feedback regulation of ATF6-mediated growth.

Our study describes a mechanism whereby ATF6 matches protein synthesis with folding in times of increased growth; since this constitutes a positive feedback mechanism, we reason that there must also be mechanisms that interrupt this feedback, thereby limiting the rate of growth driven by the ATF6-Rheb-mTORC1 axis. One such mechanism might involve Rheb itself, which has been shown to activate PERK[48]. Mechanisms such as this underscore the complexities of proteostasis, raising questions about how Rheb switches from protein synthesis activator to inhibitor.

Conclusions.

The results of our study firmly place ATF6 in a critical position as a determinant of cardiac growth (Fig. 8A). Moreover, since ATF6 is ubiquitously expressed, our findings underscore the widespread importance of the ATF6-Rheb-mTORC1-growth signaling axis described here in non-cardiac cells and tissues in addition to the heart.

Supplementary Material

Refer to Web version on PubMed Central for supplementary material.

ACKNOWLEDGMENTS

We thank Dr. Gokhan S. Hotamisligil (Harvard T.H. Chan School of Public Health, Boston, MA) for the ATF6$\alpha^{fl/fl}$ mice.

SOURCES OF FUNDING

EAB American Heart Association (17PRE33670796), the Rees-Stealy Research Foundation and SDSU Heart Institute, the Inamori Foundation, and the ARCS Foundation, Inc., San Diego Chapter.

CH Boehringer Ingelheim Fonds Travel Grant, the DZHK Mobilitätsprogramm and the Deutsche Herzstiftung

OJM the DZHK and by the BMBF (German Ministry of Education and Research)

SD was supported by an Excellence Grant from the German Centre for Cardiovascular Research (DZHK) and Department of Cardiology, Angiology, and Pneumology, University Hospital Heidelberg.

CCG by (NIH) grants R01 HL75573, R01 HL104535, and P01 HL085577.

Nonstandard Abbreviations and Acronyms:

AAV	adeno-associated virus
AdV	adenovirus
ANOVA	analysis of variance
ATF6	activating transcription factor 6 alpha
ATF6 cKO	ATF6 alpha conditional knockou
Cat	Catalase
ER	endoplasmic reticulum
Grp78	78 kilodalton glucose-regulated protein, Hapa5
HR	heart rate
HW	heart weight
ICF	immunocytofluorescence
LV	left ventricle
LVEDV	left ventricular end diastolic volume
LVESV	left ventricular end systolic volume
LVIDD	left ventricular inner diameter in diastole
LVIDS	left ventricular inner diameter in systole
PWTD	left ventricular posterior wall thickness in diastole
PWTS	left ventricular posterior wall thickness in systole
Rheb	Ras homologue enriched in brain
SR	sarcoplasmic reticulum
TAC	transverse aortic constriction
TL	tibia length
TM	tunicamycin
UPR	unfolded protein response

REFERENCES

1. Balch WE, Morimoto RI, Dillin A and Kelly JW. Adapting proteostasis for disease intervention. Science. 2008;319:916–9. [PubMed: 18276881]
2. Glembotski CC. Roles for the sarco-/endoplasmic reticulum in cardiac myocyte contraction, protein synthesis, and protein quality control. Physiology (Bethesda). 2012;27:343–50. [PubMed: 23223628]
3. Gidalevitz T, Stevens F and Argon Y. Orchestration of secretory protein folding by ER chaperones. Biochim Biophys Acta. 2013;1833:2410–24. [PubMed: 23507200]
4. Glembotski CC. Roles for ATF6 and the sarco/endoplasmic reticulum protein quality control system in the heart. Journal of Molecular and Cellular Cardiology. 2014;71:11–15. [PubMed: 24140798]
5. Arrieta A, Blackwood EA and Glembotski CC. ER Protein Quality Control and the Unfolded Protein Response in the Heart. Curr Top Microbiol Immunol. 2017.
6. Zhu C, Johansen FE and Prywes R. Interaction of ATF6 and serum response factor. Mol Cell Biol. 1997;17:4957–66. [PubMed: 9271374]
7. Haze K, Yoshida H, Yanagi H, Yura T and Mori K. Mammalian transcription factor ATF6 is synthesized as a transmembrane protein and activated by proteolysis in response to endoplasmic reticulum stress. Mol Biol Cell. 1999;10:3787–99. [PubMed: 10564271]
8. Luckey SW, Walker LA, Smyth T, Mansoori J, Messmer-Kratzsch A, Rosenzweig A, Olson EN and Leinwand LA. The role of Akt/GSK-3beta signaling in familial hypertrophic cardiomyopathy. J Mol Cell Cardiol. 2009;46:739–47. [PubMed: 19233194]
9. Bernardo BC and McMullen JR. Molecular Aspects of Exercise-induced Cardiac Remodeling. Cardiol Clin. 2016;34:515–530. [PubMed: 27692221]
10. Zhang D, Contu R, Latronico MV, Zhang J, Rizzi R, Catalucci D, Miyamoto S, Huang K, Ceci M, Gu Y, Dalton ND, Peterson KL, Guan KL, Brown JH, Chen J, Sonenberg N and Condorelli G. MTORC1 regulates cardiac function and myocyte survival through 4E-BP1 inhibition in mice. J Clin Invest. 2010;120:2805–16. [PubMed: 20644257]
11. Shende P, Plaisance I, Morandi C, Pellieux C, Berthonneche C, Zorzato F, Krishnan J, Lerch R, Hall MN, Ruegg MA, Pedrazzini T and Brink M. Cardiac raptor ablation impairs adaptive hypertrophy, alters metabolic gene expression, and causes heart failure in mice. Circulation. 2011;123:1073–82. [PubMed: 21357822]
12. Tamai T, Yamaguchi O, Hikoso S, Takeda T, Taneike M, Oka T, Oyabu J, Murakawa T, Nakayama H, Uno Y, Horie K, Nishida K, Sonenberg N, Shah AM, Takeda J, Komuro I and Otsu K. Rheb (Ras homologue enriched in brain)-dependent mammalian target of rapamycin complex 1 (mTORC1) activation becomes indispensable for cardiac hypertrophic growth after early postnatal period. J Biol Chem. 2013;288:10176–87. [PubMed: 23426372]
13. Volkers M, Toko H, Doroudgar S, Din S, Quijada P, Joyo AY, Ornelas L, Joyo E, Thuerauf DJ, Konstandin MH, Gude N, Glembotski CC and Sussman MA. Pathological hypertrophy amelioration by PRAS40-mediated inhibition of mTORC1. Proc Natl Acad Sci U S A. 2013;110:12661–6. [PubMed: 23842089]
14. Wu X, Cao Y, Nie J, Liu H, Lu S, Hu X, Zhu J, Zhao X, Chen J, Chen X, Yang Z and Li X. Genetic and pharmacological inhibition of Rheb1-mTORC1 signaling exerts cardioprotection against adverse cardiac remodeling in mice. Am J Pathol. 2013;182:2005–14. [PubMed: 23567640]
15. Sciarretta S, Forte M, Frati G and Sadoshima J. New Insights Into the Role of mTOR Signaling in the Cardiovascular System. Circ Res. 2018;122:489–505. [PubMed: 29420210]
16. Sancak Y, Peterson TR, Shaul YD, Lindquist RA, Thoreen CC, Bar-Peled L and Sabatini DM. The Rag GTPases bind raptor and mediate amino acid signaling to mTORC1. Science. 2008;320:1496–501. [PubMed: 18497260]
17. Duran RV and Hall MN. Regulation of TOR by small GTPases. EMBO Rep. 2012;13:121–8. [PubMed: 22240970]
18. Betz C and Hall MN. Where is mTOR and what is it doing there? J Cell Biol. 2013;203:563–74. [PubMed: 24385483]

19. Tee AR, Manning BD, Roux PP, Cantley LC and Blenis J. Tuberous sclerosis complex gene products, Tuberin and Hamartin, control mTOR signaling by acting as a GTPase-activating protein complex toward Rheb. Curr Biol. 2003;13:1259–68. [PubMed: 12906785]
20. Engin F, Yermalovich A, Nguyen T, Hummasti S, Fu W, Eizirik DL, Mathis D and Hotamisligil GS. Restoration of the unfolded protein response in pancreatic beta cells protects mice against type 1 diabetes. Sci Transl Med. 2013;5:211–156.
21. Wang Y, Zhang Y, Ding G, May HI, Xu J, Gillette TG, Wang H and Wang ZV. Temporal dynamics of cardiac hypertrophic growth in response to pressure overload. Am J Physiol Heart Circ Physiol. 2017;313:H1119–H1129. [PubMed: 28822967]
22. Nakamura A, Rokosh DG, Paccanaro M, Yee RR, Simpson PC, Grossman W and Foster E. LV systolic performance improves with development of hypertrophy after transverse aortic constriction in mice. Am J Physiol Heart Circ Physiol. 2001;281:H1104–12. [PubMed: 11514276]
23. Takaoka H, Esposito G, Mao L, Suga H and Rockman HA. Heart size-independent analysis of myocardial function in murine pressure overload hypertrophy. Am J Physiol Heart Circ Physiol. 2002;282:H2190–7. [PubMed: 12003828]
24. Harvey PA and Leinwand LA. The cell biology of disease: cellular mechanisms of cardiomyopathy. J Cell Biol. 2011;194:355–65. [PubMed: 21825071]
25. Allen DL, Harrison BC, Maass A, Bell ML, Byrnes WC and Leinwand LA. Cardiac and skeletal muscle adaptations to voluntary wheel running in the mouse. J Appl Physiol (1985) 2001;90:1900–8.
26. Chung E, Heimiller J and Leinwand LA. Distinct cardiac transcriptional profiles defining pregnancy and exercise. PLoS One. 2012;7:e42297. [PubMed: 22860109]
27. Bernardo BC, Weeks KL, Pretorius L and McMullen JR. Molecular distinction between physiological and pathological cardiac hypertrophy: experimental findings and therapeutic strategies. Pharmacol Ther. 2010;128:191–227. [PubMed: 20438756]
28. Martindale JJ, Fernandez R, Thuerauf D, Whittaker R, Gude N, Sussman MA and Glembotski CC. Endoplasmic reticulum stress gene induction and protection from ischemia/reperfusion injury in the hearts of transgenic mice with a tamoxifen-regulated form of ATF6. Circ Res. 2006;98:1186–93. [PubMed: 16601230]
29. Simpson P Stimulation of hypertrophy of cultured neonatal rat heart cells through an alpha 1-adrenergic receptor and induction of beating through an alpha 1- and beta 1-adrenergic receptor interaction. Evidence for independent regulation of growth and beating. Circ Res. 1985;56:884–94. [PubMed: 2988814]
30. Basso AD, Mirza A, Liu G, Long BJ, Bishop WR and Kirschmeier P. The farnesyl transferase inhibitor (FTI) SCH66336 (lonafarnib) inhibits Rheb farnesylation and mTOR signaling. Role in FTI enhancement of taxane and tamoxifen anti-tumor activity. J Biol Chem. 2005;280:31101–8. [PubMed: 16006564]
31. Okada K, Minamino T, Tsukamoto Y, Liao Y, Tsukamoto O, Takashima S, Hirata A, Fujita M, Nagamachi Y, Nakatani T, Yutani C, Ozawa K, Ogawa S, Tomoike H, Hori M and Kitakaze M. Prolonged endoplasmic reticulum stress in hypertrophic and failing heart after aortic constriction: possible contribution of endoplasmic reticulum stress to cardiac myocyte apoptosis. Circulation. 2004;110:705–12. [PubMed: 15289376]
32. Sari FR, Widyantoro B, Thandavarayan RA, Harima M, Lakshmanan AP, Zhang S, Muslin AJ, Suzuki K, Kodama M and Watanabe K. Attenuation of CHOP-mediated myocardial apoptosis in pressure-overloaded dominant negative p38alpha mitogen-activated protein kinase mice. Cell Physiol Biochem. 2011;27:487–96. [PubMed: 21691066]
33. Park CS, Cha H, Kwon EJ, Sreenivasaiah PK and Kim DH. The chemical chaperone 4-phenylbutyric acid attenuates pressure-overload cardiac hypertrophy by alleviating endoplasmic reticulum stress. Biochem Biophys Res Commun. 2012;421:578–84. [PubMed: 22525677]
34. Liu X, Kwak D, Lu Z, Xu X, Fassett J, Wang H, Wei Y, Cavener DR, Hu X, Hall J, Bache RJ and Chen Y. Endoplasmic reticulum stress sensor protein kinase R-like endoplasmic reticulum kinase (PERK) protects against pressure overload-induced heart failure and lung remodeling. Hypertension. 2014;64:738–44. [PubMed: 24958502]

35. Vekich JA, Belmont PJ, Thuerauf DJ and Glembotski CC. Protein disulfide isomerase-associated 6 is an ATF6-inducible ER stress response protein that protects cardiac myocytes from ischemia/reperfusion-mediated cell death. J Mol Cell Cardiol. 2012;53:259–67. [PubMed: 22609432]
36. Wu J, Ruas JL, Estall JL, Rasbach KA, Choi JH, Ye L, Bostrom P, Tyra HM, Crawford RW, Campbell KP, Rutkowski DT, Kaufman RJ and Spiegelman BM. The unfolded protein response mediates adaptation to exercise in skeletal muscle through a PGC-1alpha/ATF6alpha complex. Cell Metab. 2011;13:160–9. [PubMed: 21284983]
37. Misra J, Kim DK, Choi W, Koo SH, Lee CH, Back SH, Kaufman RJ and Choi HS. Transcriptional cross talk between orphan nuclear receptor ERRgamma and transmembrane transcription factor ATF6alpha coordinates endoplasmic reticulum stress response. Nucleic Acids Res. 2013;41:6960–74. [PubMed: 23716639]
38. Tam AB, Roberts LS, Chandra V, Rivera IG, Nomura DK, Forbes DJ and Niwa M. The UPR Activator ATF6 Responds to Proteotoxic and Lipotoxic Stress by Distinct Mechanisms. Dev Cell. 2018;46:327–343 e7. [PubMed: 30086303]
39. Yamagata K, Sanders LK, Kaufmann WE, Yee W, Barnes CA, Nathans D and Worley PF. rheb, a growth factor- and synaptic activity-regulated gene, encodes a novel Ras-related protein. J Biol Chem. 1994;269:16333–9. [PubMed: 8206940]
40. Potheraveedu VN, Schopel M, Stoll R and Heumann R. Rheb in neuronal degeneration, regeneration, and connectivity. Biol Chem. 2017;398:589–606. [PubMed: 28212107]
41. Heard JJ, Fong V, Bathaie SZ and Tamanoi F. Recent progress in the study of the Rheb family GTPases. Cell Signal. 2014;26:1950–7. [PubMed: 24863881]
42. Goorden SM, Hoogeveen-Westerveld M, Cheng C, van Woerden GM, Mozaffari M, Post L, Duckers HJ, Nellist M and Elgersma Y. Rheb is essential for murine development. Mol Cell Biol. 2011;31:1672–8. [PubMed: 21321084]
43. Wang Y, Huang BP, Luciani DS, Wang X, Johnson JD and Proud CG. Rheb activates protein synthesis and growth in adult rat ventricular cardiomyocytes. J Mol Cell Cardiol. 2008;45:812–20. [PubMed: 18722381]
44. Sciarretta S, Zhai P, Shao D, Maejima Y, Robbins J, Volpe M, Condorelli G and Sadoshima J. Rheb is a critical regulator of autophagy during myocardial ischemia: pathophysiological implications in obesity and metabolic syndrome. Circulation. 2012;125:1134–46. [PubMed: 22294621]
45. Cao Y, Tao L, Shen S, Xiao J, Wu H, Li B, Wu X, Luo W, Xiao Q, Hu X, Liu H, Nie J, Lu S, Yuan B, Han Z, Xiao B, Yang Z and Li X. Cardiac ablation of Rheb1 induces impaired heart growth, endoplasmic reticulum-associated apoptosis and heart failure in infant mice. Int J Mol Sci. 2013;14:24380–98. [PubMed: 24351823]
46. Schewe DM and Aguirre-Ghiso JA. ATF6alpha-Rheb-mTOR signaling promotes survival of dormant tumor cells in vivo. Proc Natl Acad Sci U S A. 2008;105:10519–24. [PubMed: 18650380]
47. Fernandez-Fernandez MR, Ferrer I and Lucas JJ. Impaired ATF6alpha processing, decreased Rheb and neuronal cell cycle re-entry in Huntington's disease. Neurobiol Dis. 2011;41:23–32. [PubMed: 20732420]
48. Tyagi R, Shahani N, Gorgen L, Ferretti M, Pryor W, Chen PY, Swarnkar S, Worley PF, Karbstein K, Snyder SH and Subramaniam S. Rheb Inhibits Protein Synthesis by Activating the PERK-eIF2alpha Signaling Cascade. Cell Rep. 2015.

NOVELTY AND SIGNFICANCE

What Is Known?

- Cardiac myocytes in the heart exhibit adaptive hypertrophic growth in response to pathological and physiological conditions, both of which activate mTORC1 signaling and increase protein synthesis, critical drivers of cardiac growth.
- Increased protein synthesis places demands on the protein-folding machinery in cardiac myocytes, leading to some protein misfolding, which activates the transcription factor, ATF6, which regulates a gene program that fortifies cellular protein-folding capacity.

What new information does this article contribute?

- Selective deletion of ATF6 in cardiac myocytes of mice impaired mTORC1 signaling, protein synthesis and cardiac hypertrophy, demonstrating that ATF6 is required for heart growth.
- Selective activation of ATF6 in mouse hearts induced *RHEB*, a required activator of mTORC1 and protein synthesis, identifying ATF6 as a previously unrecognized link between pathological and physiological growth stimuli and mTOR-mediated increases in protein synthesis, protein folding and cardiac growth.

ER stress impairs ER protein folding, which activates the transcription factor, ATF6, an inducer of genes that restores ER protein folding. We hypothesized that increased protein synthesis during cardiac hypertrophy might challenge protein folding by ER, leading toactivation of ATF6. We found that ATF6 was activated in mice subjected to pathological and physiological growth conditions that promote adaptive cardiac myocyte hypertrophy. Cardiac myocyte-specific deletion of ATF6 blunted adaptive cardiac myocyte hypertrophy, while ectopic expression of ATF6 enhanced the hypertrophic response. Here, ATF6 was found to promote the induction of *RHEB,* an obligate activator of mTORC1, a known regulator of protein synthesis and cellular growth. Ectopic expression of *RHEB* restored cardiac growth to ATF6 cKO mice. ATF6 induced *RHEB* in response to growth factors, but not in response to other activators of ATF6 that do not induce growth, indicating that ATF6 target gene induction is stress-specific. Thus, ATF6 is a newly identified, essential member of mTORC1-mediated growth signaling in the heart. Moreover, since ATF6 is ubiquitously expressed, our findings underscore the potential widespread importance of this new ATF6-Rheb-mTORC1-growth signaling axis in non-cardiac cells and tissues in addition to the heart.

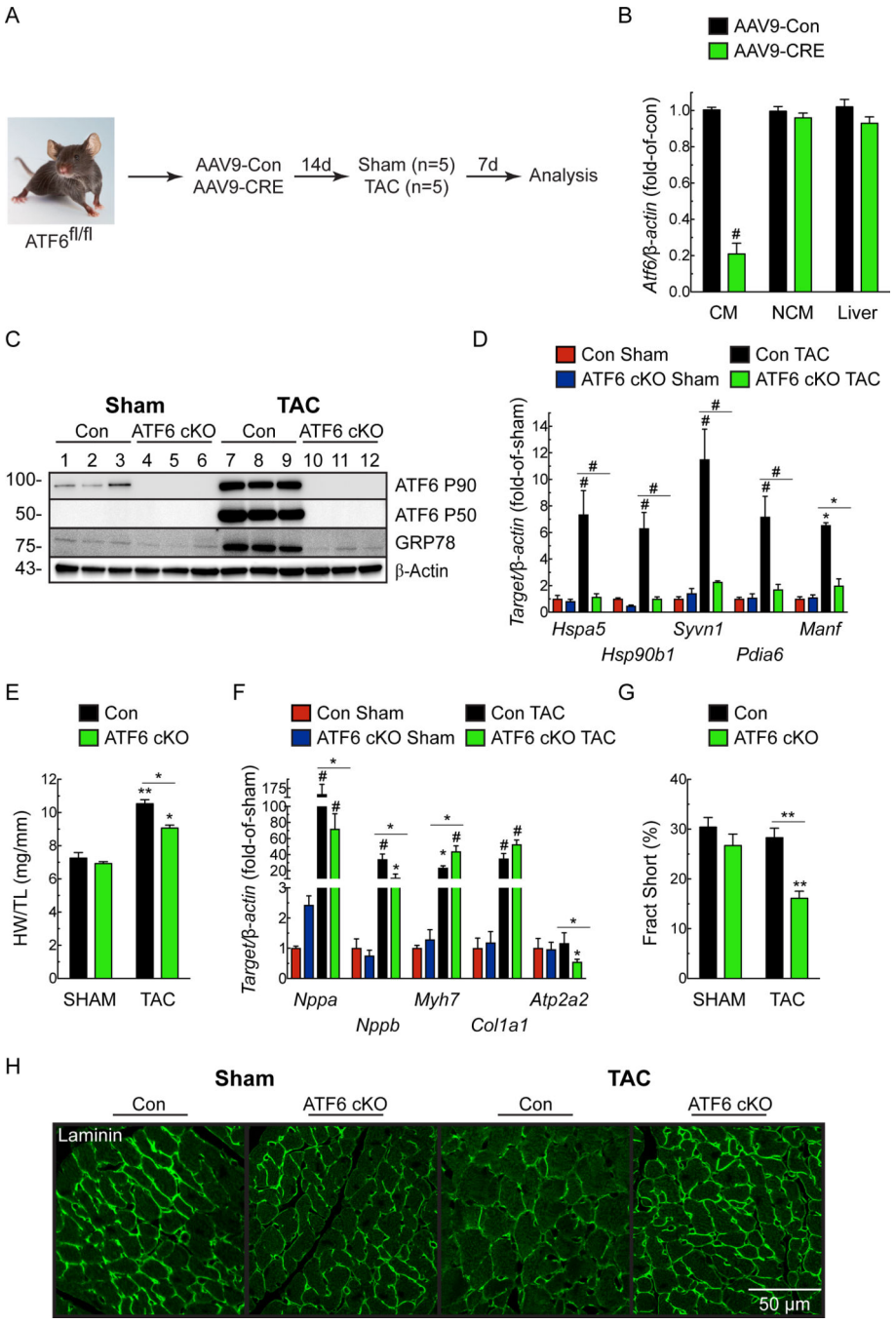

Figure 1. Effect of cardiac myocyte-specific ATF6 gene deletion in hearts of mice subjected to TAC.

A, Protocol for AAV9 administration to ATF6$^{fl/fl}$ mice and TAC. **B,** ATF6 mRNA levels determined by qRT-PCR on isolated cardiac myocytes (CM), non-cardiac myocytes (NCM), and liver extracts from ATF6$^{fl/fl}$ mice injected with AAV9-Con (Con) or AAV9-CRE (i.e. ATF6 cKO) n=3. **C,** Immunoblot of LV extracts from Con or ATF6 cKO mice. **D,** mRNA for ATF6 target genes determined by qRT-PCR. **E,** Heart weight/tibia lengths (HW/TL). **F,** mRNA levels for fetal genes determined by qRT-PCR. *Nppa*, natriuretic peptide A); *Nppb*,

natriuretic peptide B); *Myh7*, β-myosin heavy chain; *Col1a1*, Collagen 1A1; *Atp2a2*, Serca2a. **G,** Fractional shortening (%), determined by echocardiography, see Online Table I. **H,** Confocal immunocytofluorescence microscopy (ICF) analysis of mouse heart sections for laminin (green). Data are mean ± SEM. $^{*}P \leq 0.05$, $^{**}P \leq 0.01$, $^{\#}P \leq 0.001$ different from Con Sham, or from the value shown by the bar.

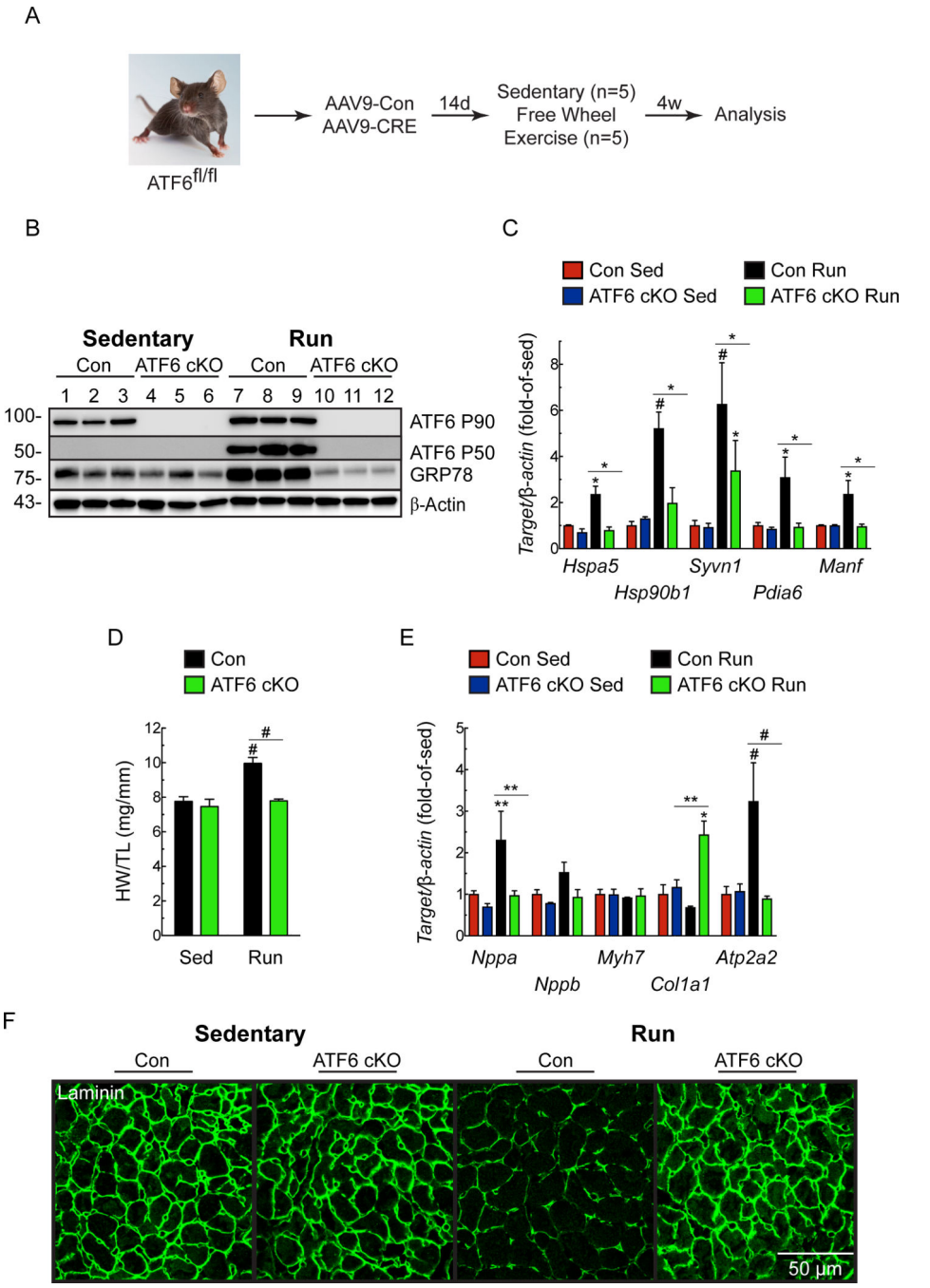

Figure 2. Effect of cardiac myocyte-specific ATF6 gene deletion in hearts of mice subjected to free wheel exercise.

A, Protocol for AAV9 administration to ATF6$^{fl/fl}$ mice and free wheel exercise. **B,** Immunoblot of LV extracts from Con or ATF6 cKO mice. **C,** mRNA levels for ATF6 target genes determined by qRT-PCR. **D,** Heart weights/tibia lengths (HW/TL). **E,** mRNA levels for fetal genes determined by qRT-PCR. **F,** ICF analysis of mouse heart sections for laminin (green). Data are mean ± SEM. *$P \leq 0.05$, **$P \leq 0.01$, $^{\#}P \leq 0.001$. Echocardiography details are in Online Table II.

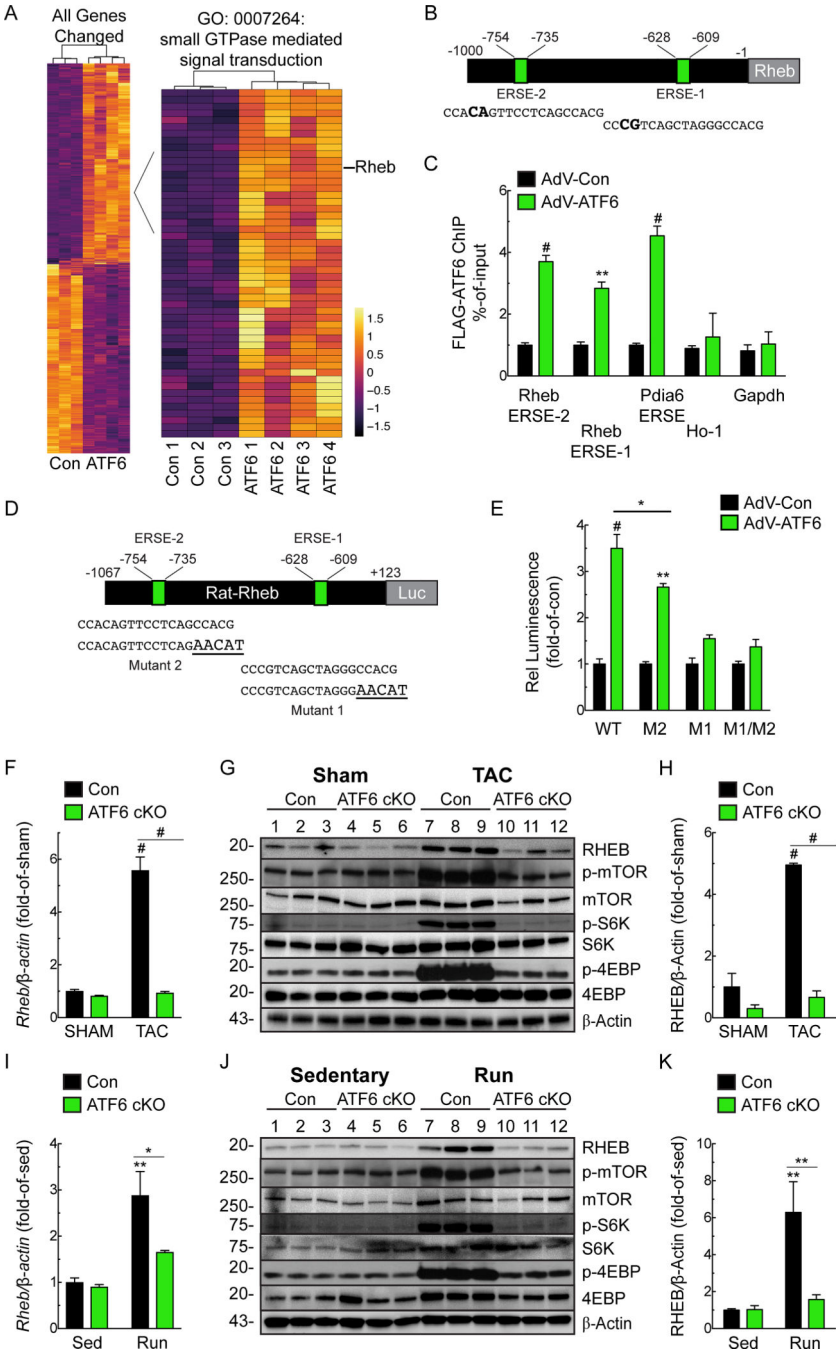

Figure 3. Regulation of Rheb Expression by ATF6.

A, Heat map of transcript profiling showing z-score-transformed RPKM values (Reads Per Kilobase per Million mapped reads) with hierarchical clustering of transcripts of control and ATF6 transgenic mouse hearts. Differentially expressed genes with *p* values and FDR ≤0.05 and a subset of genes annotated with term GO:0007264 are shown. All the genes increased or decreased by ATF6 are in Online Table III. **B,** Locations of consensus ATF6-binding motifs, i.e. ER stress response elements 1 and 2 (ERSE-1 and 2) and their sequences in the *RHEB* gene 5'-flanking region. Nucleotide differences from canonical ERSE elements are

bold. **C,** Neonatal rat ventricular myocytes (NRVM) were infected with AdV encoding control or FLAG-ATF6(1–373) [active form], and then ATF6 binding to endogenous ERSE-1 or ERSE-2, as well as to the endogenous *PDIA6* ERSE, used here as a positive control, and the negative control targets heme oxygenase 1 (*ho-1*) and *gapdh* were examined by chromatin immunoprecipitation (ChIP) (n=3). **D,** Locations of ERSE-1 and 2 in the *RHEB* 5'-flanking region, their sequences (lower case), and the mutations that were made (bold and upper case). **E,** NRVM were transfected with rat-*rheb*(−1067/+123)-Luc WT, M2, M1 or M1/M2 then infected with AdV FLAG-ATF6(1–373),. Then, 48h later, luciferase activity was measured in extracts (n=6). **F-H,** mRNA for *RHEB* determined by qRT-PCR (**F**) and Rheb protein and mTOR pathway components measured by immunoblots (**G**) and quantified by densitometry (**H**) from Con or ATF6 cKO mouse heart extracts after 7 days of Sham or TAC. **I-K,** mRNA for *RHEB* determined by qRT-PCR (**I**) and Rheb protein and mTOR pathway components immunoblots (**J**) and quantified by densitometry (**K**) from Con or ATF6 cKO mouse heart extracts after 4 weeks of sedentary or free wheel exercise (Run). Data are mean ± SEM. $*P \leq 0.05$, $**P \leq 0.01$, $^{\#}P \leq 0.001$.

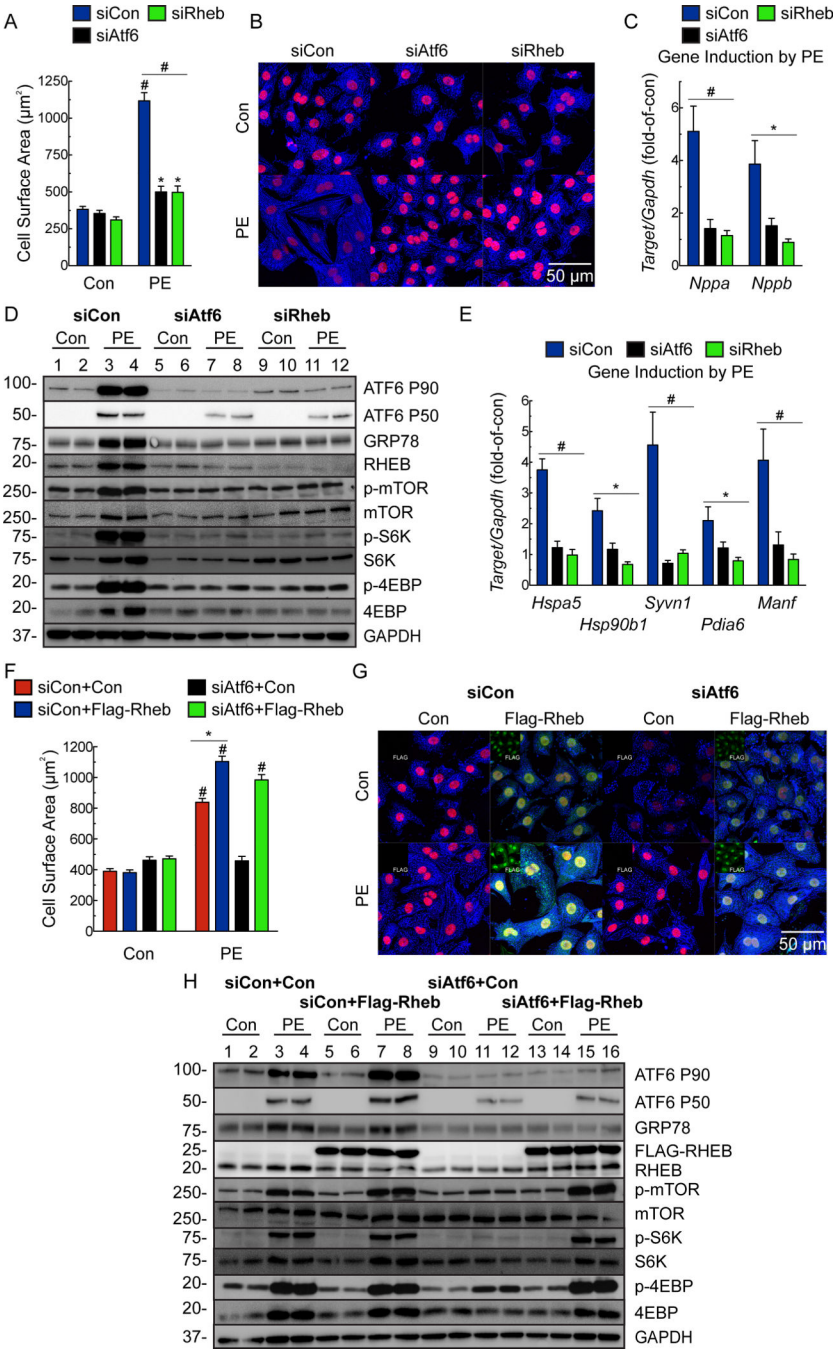

Figure 4. Effects of *ATF6*- and *RHEB* knockdown and ectopic Rheb expression on phenylephrine-induced hypertrophy in cultured cardiac myocytes.

A-E, NRVM were transfected with a nontargeted siRNA (siCon) or with siRNAs targeted to either rat *ATF6* (siAtf6) or *RHEB* (siRheb), and then treated ± phenylephrine (PE; 50μM) for 48 hours. **A,** Cell surface area was determined by photomicroscopy and morphometry (n=6). **B,** ICF of NRVM for α-actinin (blue) and TOPRO-3 (red). Bar = 50μm. **C,** qRT-PCR examination of *Nppa* and *Nppb*. Values are expressed as fold-of-control cardiac myocytes in the absence of PE (n=6). **D,** Immunoblot of NRVM. **E,** mRNA for ATF6 target genes

determined by qRT-PCR. Values are expressed as fold-of-control myocytes in the absence of PE (n=3). **F-H,** NRVM were transfected with a control plasmid or a plasmid encoding Flag-Rheb and either siCon or siAtf6, followed by treatment ± PE for 48 hours. Cell surface area (**F**) was determined by morphometry after ICF (**G**). NRVM were stained for FLAG (green; isolated channel displayed in inset), α-actinin (blue), and TOPRO-3 (red). Bar = 50μm. Only FLAG-positive cells were used for cell surface area analysis (n=3). **H,** Immunoblot of NRVM. Data are mean ± SEM. $*P \leq 0.05$, $**P \leq 0.01$, $^{\#}P \leq 0.001$.

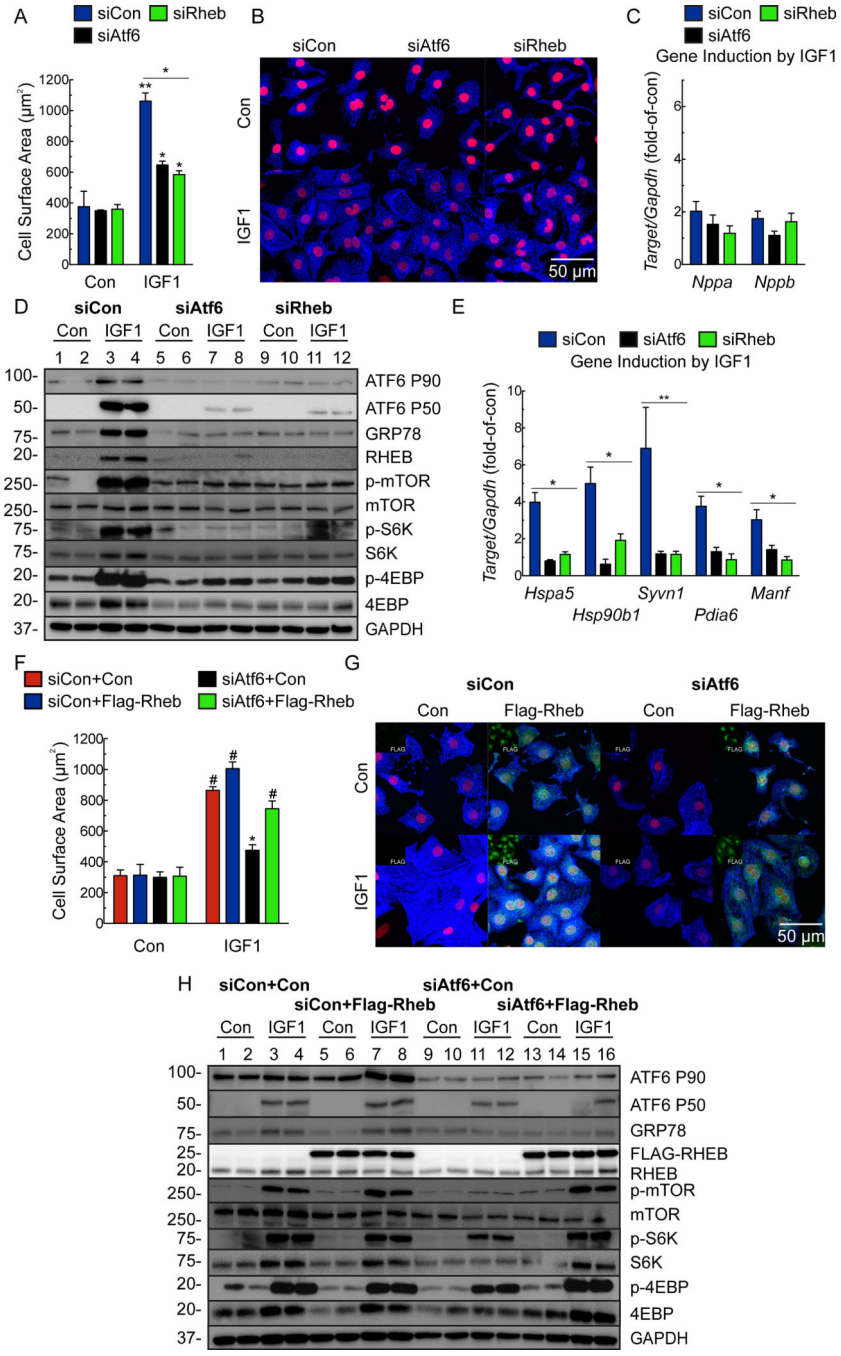

Figure 5. Effects of *ATF6*- and *RHEB* knockdown and ectopic Rheb expression on insulin like growth factor 1-induced hypertrophy in cultured cardiac myocytes.

A-E, NRVM were transfected with siCon, siAtf6 or siRheb, then treated ± IGF1 (100ng/ml) for 48 hours. **A,** Cell surface area was determined by was determined by morphometry after ICF (n=6). **B,** ICF of NRVM for α-actinin (blue) and TOPRO-3 (red). Bar = 50μm. **C,** qRT-PCR for *Nppa* and *Nppb*. Values are fold-of-control myocytes in the absence of IGF1 (n=6). **D,** Immunoblot of NRVM. **E,** mRNA levels of ATF6 target genes determined by qRT-PCR. Values are fold-of-control myocytes in the absence of IGF1 (n=3). **F-H,** NRVM were

transfected with a control plasmid or a plasmid encoding Flag-Rheb and then either siCon or siAtf6, followed by treatment ± IGF1 for 48 hours. Cell surface area (**F**) was determined by morphometry after ICF (**G**). NRVM were stained for FLAG (green; isolated channel displayed in inset), α-actinin (blue) and TOPRO-3 (red). Bar = 50μm. Only FLAG-positive cells were used for cell surface area analysis (n=3). **H,** Immunoblot of NRVM. Data are mean ± SEM. *$P \leq 0.05$, **$P \leq 0.01$, $^{\#}P \leq 0.001$.

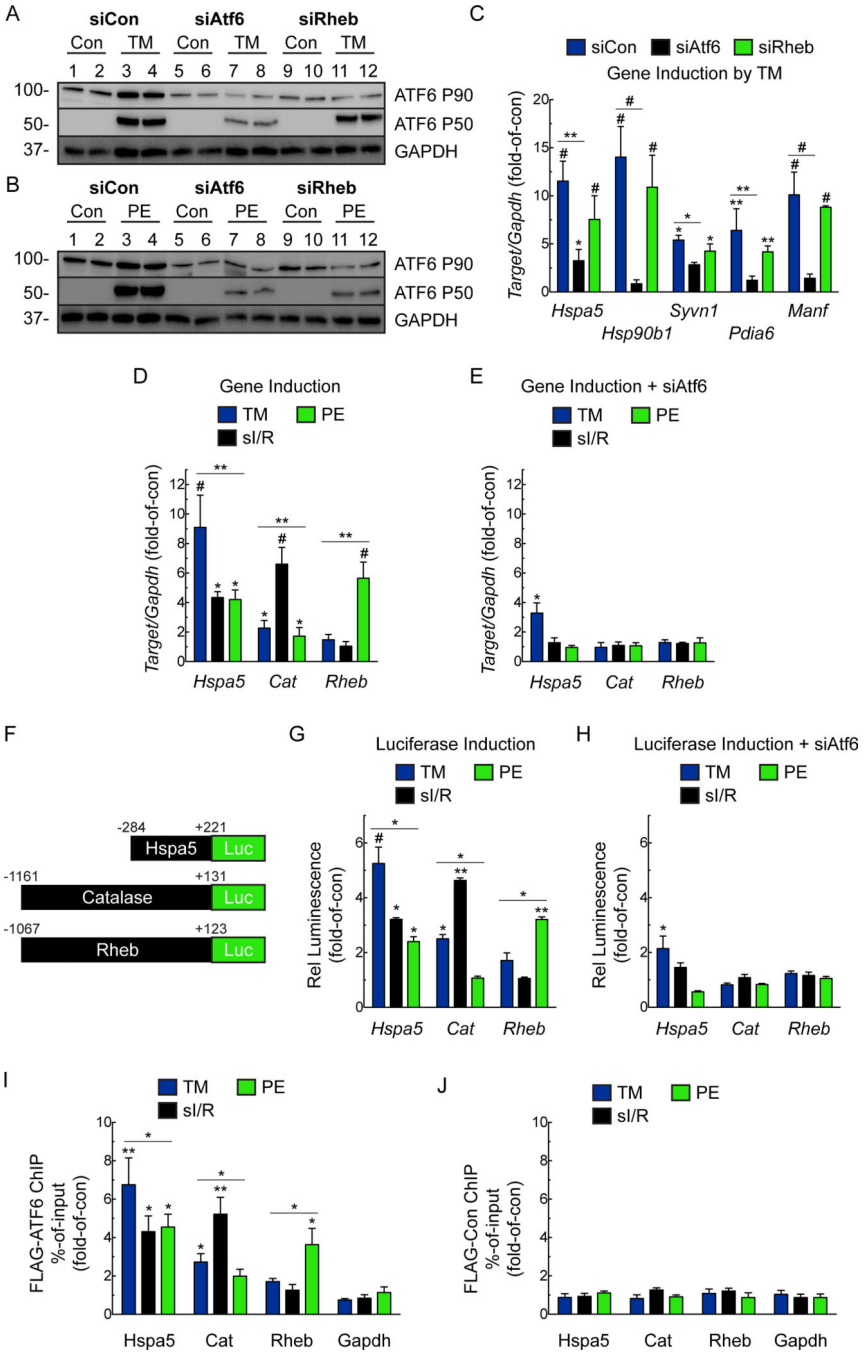

Figure 6. Examination of Rheb Requirement for Growth-dependent but not Growth-independent Activation of the ATF6.

A-B, NRVM were transfected with siCon, siAtf6 or siRheb then treated ± tunicamycin (TM; 10μg/mL) (**A**) or PE (50μM) (**B**) for 24 hours, then analyzed for ATF6 activation by immunoblotting. **C,** mRNA levels for ATF6 target genes determined by qRT-PCR. Values are fold-of-control, i.e. not treated with TM (n=6). **D, E,** NRVM were transfected with siCon (**D**) or siAtf6 (**E**), then treated ± TM (10μg/mL), or PE (50μM) for 24 hours, or subjected to simulated ischemia/reperfusion (sI/R; 8 hours of sI, followed by 24 hours of reperfusion)

and mRNA for ATF6 target genes determined by qRT-PCR (n=6). **F,** Diagram of constructs that encode luciferase driven by the *grp78*, *catalase*, and *rheb* 5'-flanking region. **G, H,** NRVM were transfected with human-*grp78*(−284/+221)-Luc WT, rat-*catalase*(−1161/+131)-Luc WT, or rat-*rheb*(−1067/+123)-Luc WT and then transfected with siCon (**G**) or siAtf6 (**H**), then treated ± TM (10μg/mL), or PE (50μM) for 24 hours, or subjected to sI/R and luciferase activity measured in extracts (n=6). **I, J,** NRVM infected with AdV FLAG-ATF6(1–670) (**I**) or control (**J**), and then ATF6 binding to the endogenous *grp78*, *catalase*, or *rheb* genes, as well as to the negative control gene, *gapdh,* examined by ChIP under the same experimental conditions described above (n=3). Data are mean ± SEM. $^{*}P \leq 0.05$, $^{**}P \leq 0.01$, $^{\#}P \leq 0.001$.

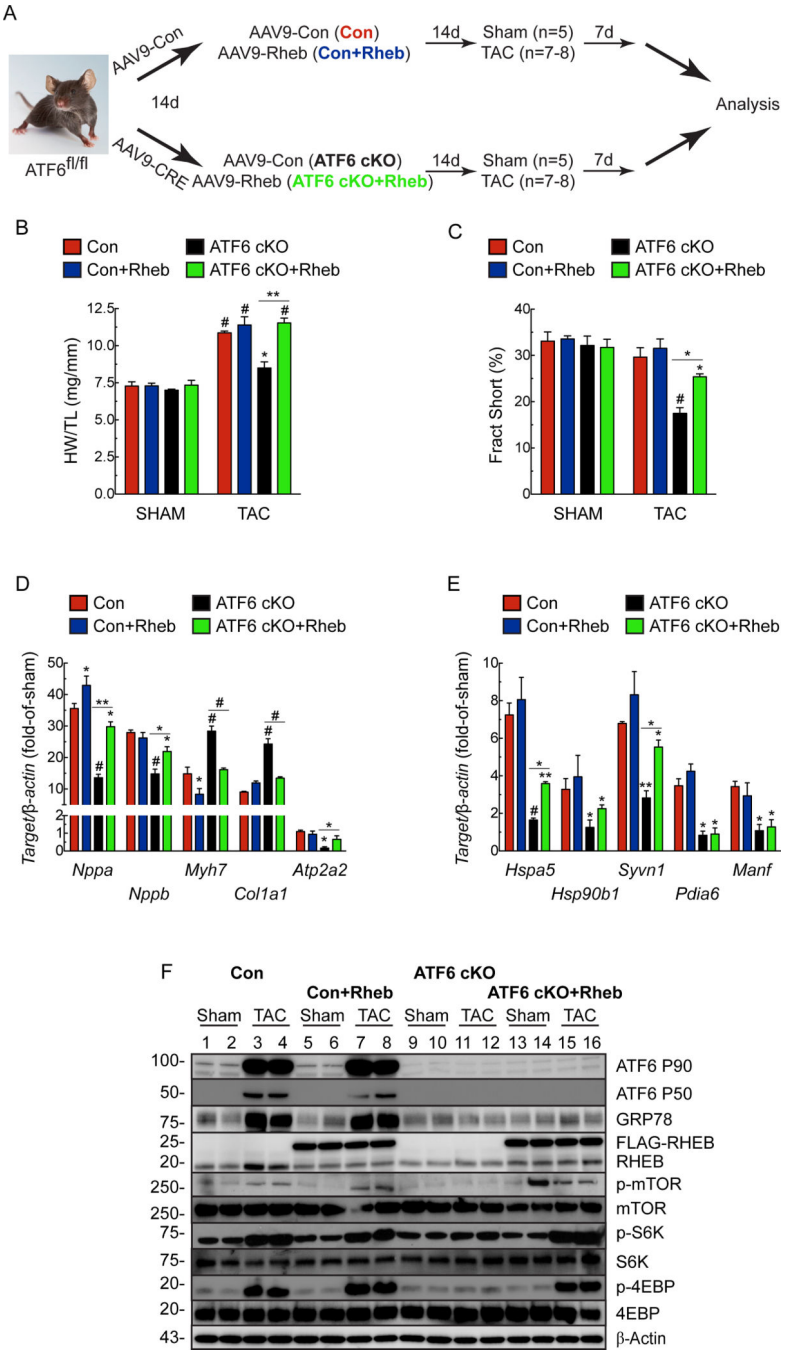

Figure 7. Effect of cardiac myocyte-specific ectopic Rheb expression in ATF6 gene deleted mouse hearts subjected to TAC.

A, Experimental protocol for AAV9 administration to ATF6$^{fl/fl}$ mice and TAC. **B,** Heart weights/tibia lengths (HW/TL). **C,** Fractional shortening (%), as determined by echocardiography, see Online Table IV. **D,** mRNA for fetal genes determined by qRT-PCR. **E,** mRNA for ATF6 target genes determined by qRT-PCR. **F,** Immunoblots of LV extracts. Data are mean ± SEM. *$P \leq 0.05$, **$P \leq 0.01$, $^{\#}P \leq 0.001$.

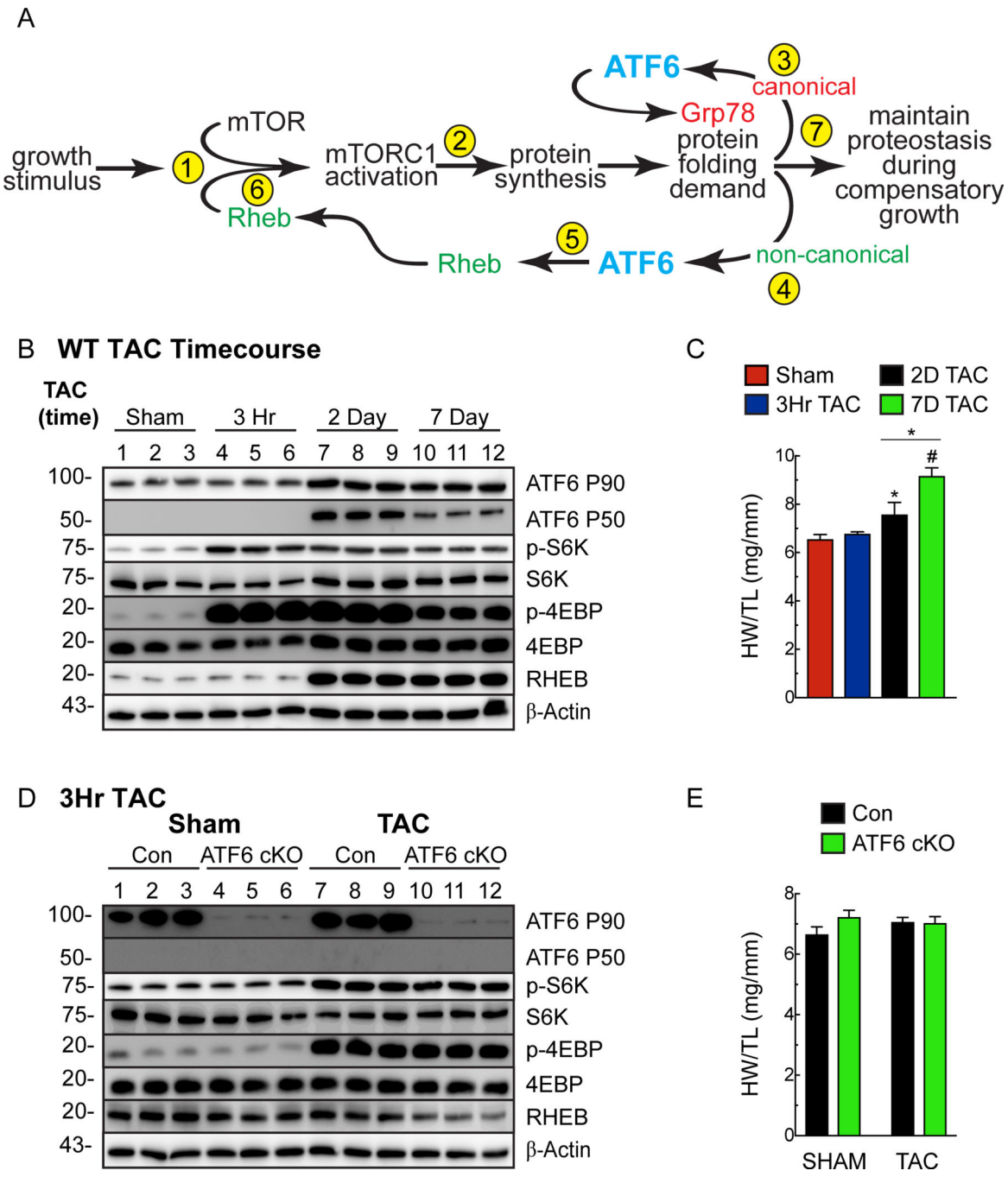

Figure 8. Mechanism whereby ATF6 acts as a nodal regulator of both protein synthesis and protein folding during cardiac hypertrophy.

A, Shown are the temporal sequence of steps involved in mediating the initial (Steps 1–4) and sustained (Steps 5–7) aspects of growth and the interdependent roles of mTORC1 and ATF6. **B, C,** Immunoblot of LV extracts (**B**) and heart weights/tibia lengths (HW/TL) (**C**) from WT mice subjected to TAC for 3 hours, 2 days, or 7 days. Echocardiography details in Online Table V. **D, E,** Immunoblot of LV extracts (**D**) and heart weights/tibia lengths

(HW/TL) (**E**) from Con or ATF6 cKO mice subjected to 3 hours of TAC. Echocardiography details in Online Table VI. Data are mean ± SEM. *$P \leq 0.05$, $^{\#}P \leq 0.001$.